

Article

One-Dimensional Chain-Type Dicopper Coordination Polymer Linked by 1,4-Di(4-pyridyl)benzene; Synthesis, Crystal Structure, Magnetic Property, and Gas-Adsorption Property

Natsumi Yano ¹, Makoto Handa ^{1,*}, Minoru Mitsumi ² and Yusuke Kataoka ^{1,*}

¹ Department of Chemistry, Interdisciplinary Faculty of Science and Engineering, Shimane University, 1060, Nishikawatsu, Matsue, Shimane 690-8504, Japan; s179802@matsu.shimane-u.ac.jp

² Department of Chemistry, Faculty of Science, Okayama University of Science, 1-1, Ridaicho, Kita-ku, Okayama 700-0005, Japan; mitsumi@chem.ous.ac.jp

* Correspondence: handam@riko.shimane-u.ac.jp (M.H.); kataoka@riko.shimane-u.ac.jp (Y.K.); Tel.: +81-852-32-6418 (M.H.); +81-852-32-6413 (Y.K.)

Received: 12 May 2018; Accepted: 8 June 2018; Published: 11 June 2018



Abstract: A one-dimensional chain-type dicopper(II) coordination polymer with 1,4-di(4-pyridyl)-benzene (dpybz), [Cu₂(O₂C-*t*Bu)₄(dpybz)] (**1**), is synthesized and characterized by single crystal X-ray diffraction, infrared spectroscopy, and CHN elemental analysis. Single crystal X-ray diffraction confirms that the one-dimensional chains of **1** are assembled with CH···π interactions at the dpybz moieties to form a brick-like porous network structure. Magnetic susceptibility measurement and broken-symmetry density functional theory (BS-DFT) calculations indicate that (i) antiferromagnetic interactions are present between two copper ions through the bridging carboxylate ligands; the observed exchange integral value (*J*) of **1** is -175.3 cm^{-1} , which is consistent with the DFT-calculated value for **1** (-174.5 cm^{-1}), and (ii) the magnetic interaction between two Cu₂ units through the dpybz ligand is negligible. N₂ adsorption measurements indicate that the porous structure of **1** is retained even after evacuation of the guest solvents from the pores of **1**, and **1** adsorbs N₂ molecules into its pores (the Langmuir surface area of **1** is estimated as 538.0 m²/g).

Keywords: paddlewheel-type complex; dicopper complex; coordination polymer; magnetic property; density functional theory calculations

1. Introduction

A paddlewheel-type dicopper (Cu₂) unit bridged by four carboxylate ([−]O₂C-R) ligands, [Cu₂(O₂C-R)₄], is well known as an important molecular skeleton in the area of coordination chemistry [1–4], because it has been widely utilized as a secondary building block (SBU) for supra-molecular cages [5], coordination polymers (CPs) [6,7] and metal–organic frameworks (MOFs) [8,9]. Current synthetic strategies for [Cu₂(O₂C-R)₄] SBU-based CPs and MOFs involve linking the Cu₂ units through organic mono- or poly-carboxylate and diimine ligands (N~N) at the equatorial and axial positions of the Cu₂ units, respectively [10,11]. For example, in 1995, Mikuriya et al. reported the synthesis and characterization of one-dimensional CPs [Cu₂(O₂C-*t*Bu)₄(N~N)], in which [Cu₂(O₂C-*t*Bu)₄] SBUs were linked by 1,4-diazabicyclo[2.2.2]octane (DABCO), pyrazine (pyz), and 4,4'-bipyridine (bpy) ligands [12]. These CPs are robust in air and occur in the crystalline state. The magnetic measurement of [Cu₂(O₂C-*t*Bu)₄(pyz)] reveals an antiferromagnetic interaction (*J* = -169.5 cm^{-1} , *g* = 2.09) between two Cu ions through four bridging carboxylate ligands. Following

this study, a one-dimensional CP, $[\text{Cu}_2(\text{O}_2\text{C-Ph})_4(\text{pyz})]$, was reported by Mori, Mikuriya, and Handa in 1999 [13]. In this CP, two phenyl groups of neighboring chains are stacked by non-covalent π - π stacking interactions to give one-dimensional uniform channels, which are suitable for N_2 gas adsorption. The channel structure in the CP is maintained, even after removal of the CH_3CN crystallization solvent molecules from the crystal by drying the sample under vacuum. Since then, although there have been many reports on the synthesis and characterization of one-dimensional CPs, DABCO, pyz, bpy and their derivative linker ligands have been commonly used in combination with paddlewheel-type dicopper complexes [14–16]. Our research is now being directed to developing the chemistry of CPs with different types of linker ligands having enlarged molecular sizes with extended π -systems, and to investigating their (self-assembled) geometries, electronic structures and functional properties [17].

In this paper, we described the synthesis, characterization, and magnetic and gas-adsorption properties of one-dimensional Cu_2 CPs with 1,4-di(4-pyridyl)benzene (dpybz; see Figure 1) as an extended N~N linker ligand, $[\text{Cu}_2(\text{O}_2\text{C-}t\text{Bu})_4(\text{dpybz})]$ (**1**). To the best of our knowledge, this is the first example of a one-dimensional Cu_2 CP with the dpybz ligand. Interestingly, one-dimensional chains of **1** were assembled and stabilized with electrostatic CH- π interactions at the dpybz moieties; no such interaction was confirmed for CPs with pyz and bpy linkers. Density functional theory (DFT) calculations were performed to give a clear insight into the structural and electronic features affecting the magnetic properties of **1**.

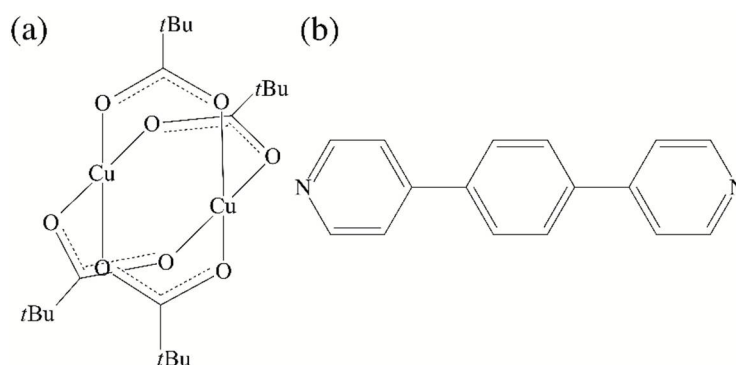


Figure 1. Molecular geometries of (a) $[\text{Cu}_2(\text{O}_2\text{C-}t\text{Bu})_4]$ and (b) dpybz.

2. Results and Discussion

2.1. Synthesis and Characterization of $[\text{Cu}_2(\text{O}_2\text{C-}t\text{Bu})_4(\text{dpybz})]$ (**1**)

Complex **1** was synthesized via a room temperature reaction between a tetrahydrofuran (THF) solution of $[\text{Cu}_2(\text{O}_2\text{C-}t\text{Bu})_4]$ (see Figure 1a) and a *N,N*-dimethylformamide (DMF) solution containing an equivalent amount of dpybz in an Erlenmeyer flask. Green crystals of **1** with a yield of 80.0%, which are suitable for single crystal X-ray diffraction measurements, were deposited on the bottom of the flask after leaving the homogeneous reaction solution for 10 days. More detailed synthetic information concerning **1** is given in Section 3.5. Elemental analysis revealed that the crystalline powder of **1**, which was obtained after heating at 353 K under vacuum for 3 h, contained no crystallization solvent and was anhydrous. In the infrared spectrum (see Figure S1), a symmetric vibration (ν_{sym}) and an asymmetric vibration (ν_{asym}) of the bridging carboxylate of **1** were observed at 1418 and 1607 cm^{-1} , respectively, similar to those of $[\text{Cu}_2(\text{O}_2\text{C-}t\text{Bu})_4]$ ($\nu_{\text{sym}} = 1418 \text{ cm}^{-1}$, $\nu_{\text{asym}} = 1578 \text{ cm}^{-1}$), indicating that **1** possessed the paddlewheel-type Cu_2 core as its SBU.

2.2. Single Crystal X-ray Diffraction

Single crystal X-ray diffraction for **1** was measured at 150 K. The crystallographic data of **1** are summarized in Table S1 in the experimental section. The diffraction analysis revealed that **1** crystallized in the monoclinic system with a space group $C 2/c$. The final refined structural model

of **1** shows that an asymmetric unit of **1** contains one Cu^{2+} ion, two $\text{O}_2\text{C}-t\text{Bu}$ anions, and one half of a dpybz ligand. This indicates that the crystallographic inversion centers of **1** were located at the midpoints of the paddlewheel-type Cu_2 unit and the dpybz ligand. Selected bond distances and angles of **1** are summarized in Table S2 in the Supplementary Materials, and expanded and packing structures of **1** are shown in Figure 2. As shown in Figure 2a, the two Cu ions in **1** were coordinated by four μ -carboxylate and one dpybz ligand. That is, **1** possessed the paddlewheel-type Cu_2 core as its SBU, and the dpybz ligand coordinated to the axial sites of the paddlewheel-type Cu_2 cores. The $\text{Cu}\cdots\text{Cu}$ distance in the paddlewheel-type Cu_2 units of **1** was 2.5938(6) Å, which was close to the typical $\text{Cu}\cdots\text{Cu}$ distances of paddlewheel-type Cu_2 complexes with analogous pyridyl ligands, such as $[\text{Cu}_2(\text{O}_2\text{C}-t\text{Bu})_4(\text{pyz})]$ (2.584(2) Å), indicating that no direct Cu–Cu bond is present between two Cu ions in **1** by judging from the similarity in the $\text{Cu}\cdots\text{Cu}$ distance between $[\text{Cu}_2(\text{O}_2\text{C}-t\text{Bu})_4(\text{pyz})]$ and **1** [12]. Thus, the primary coordination spheres of two Cu ions in **1** were in pentacoordinated environments with a square pyramidal structure. Expanding the structure of **1** showed an alternating arrangement of paddlewheel-type Cu_2 units and dpybz ligands along the $\text{Cu}\cdots\text{Cu}$ vector, confirming a one-dimensional polymeric (chain) structure of **1**. In the dpybz ligand of **1**, two pyridyl rings at both ends of dpybz were located in a coplanar arrangement; the dihedral angles defined by the pyridyl rings were 0° , whereas both those defined by pyridyl and benzene rings within the dpybz ligand were 37.15° . The Cu–N bond length in **1** was 2.156(2) Å, which was also comparable to that of $[\text{Cu}_2(\text{O}_2\text{C}-t\text{Bu})_4(\text{pyz})]$ (2.195(8) Å) [12].

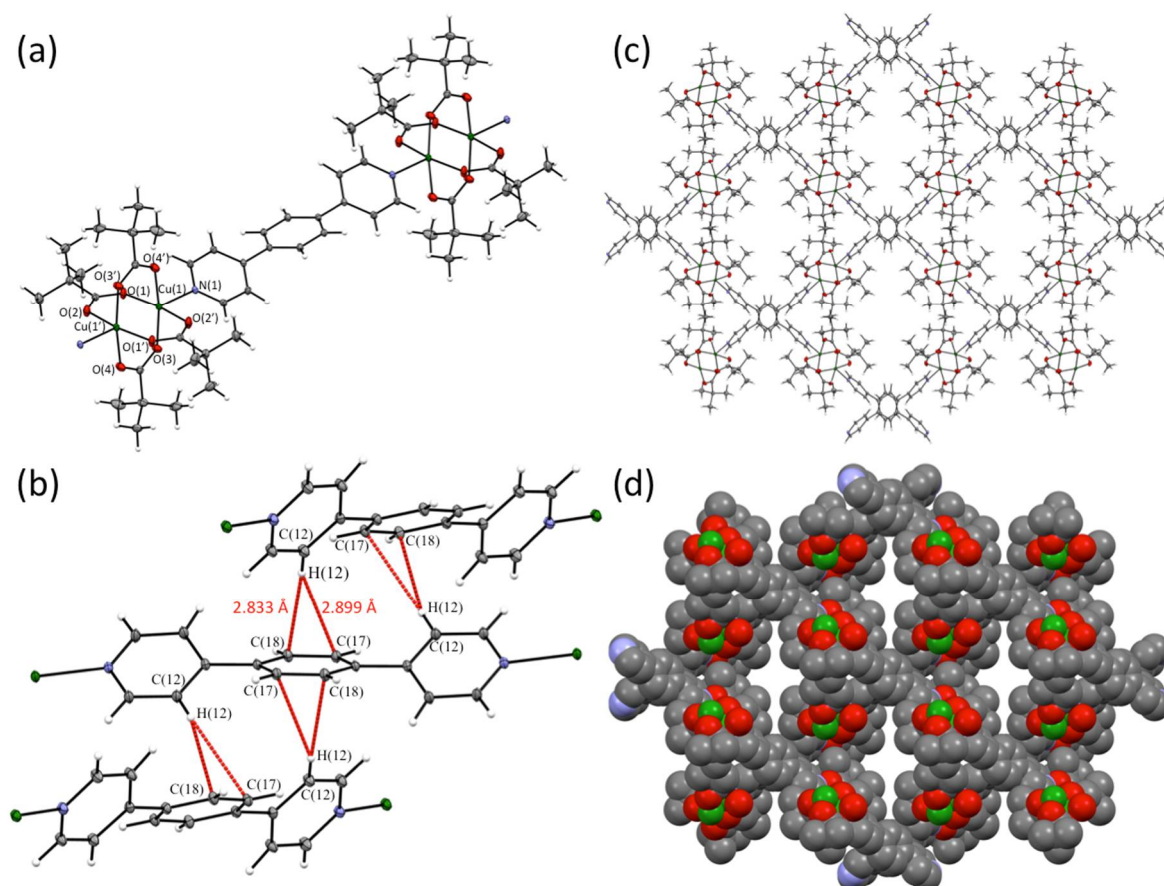


Figure 2. Crystal structure of **1**. (a) Chain structure, (b) CH- π interactions of dpybz moieties, (c) packing view along c axis, and (d) CPK model of (c). Here, thermal ellipsoids of (a–c) are drawn with 20% probability. In (d), hydrogen atoms are omitted for clarity. Green: Cu, Red: O, Gray: C, Blue: N, and White: H.

As shown in Figure 2c,d, the one-dimensional chains of **1** were assembled to form a brick-like porous network structure. Interestingly, the benzene moieties of dpybz ligands were arranged in a one-dimensional fashion along the *c* axis to form fourfold CH- π interactions with the upper and lower benzene moieties of dpybz ligands, as shown in Figure 1b. The CH(12)··· π (the midpoint of C17 and C18) distance was estimated as 2.781 Å (H(12)···C(17): 2.899 Å, H(12)···C(18): 2.833 Å), which implies the existence of CH- π interactions [18]. Two DMF guest solvent molecules in **1** were disordered and their positions could not be determined. Thus, the PLATON SQUEEZE program was applied to estimate the void volume of **1** and to eliminate the residual electron density in the pores of **1** [19]. The solvent accessible void volume of **1** was estimated as 254.2 Å³ per Cu₂ unit, which is nearly the same as the sum of the volumes of two DMF molecules (258 Å³). The void volume percentage of **1** was determined as 22.5%. The channel-like pore diameter of **1** was 5.53 × 5.05 Å² along the *c* axis, which is considered to be a preferable for gas adsorption.

2.3. Magnetic Property of **1**

For **1**, variable-temperature (VT) magnetic susceptibility measurement was performed with a SQUID magnetometer within the temperature range (2–300 K). As a comparison, the VT magnetic susceptibility of [Cu₂(O₂C-*t*Bu)₄] was also measured. Figure 3 shows the molar magnetic susceptibilities (χ_M) and effective magnetic moments (μ_{eff}) (per Cu₂ unit) of **1** and [Cu₂(O₂C-*t*Bu)₄]. At 300 K, the χ_M and μ_{eff} of **1** were 0.00143 emu mol⁻¹ and 1.85 μ_B , respectively. The μ_{eff} of **1** was within the typical range for paddlewheel-type Cu₂ complexes (1.6–1.9 μ_B) and slightly larger than that of [Cu₂(O₂C-*t*Bu)₄] (1.76 μ_B) [12,13]. When the temperature was decreased from 300 K, the μ_{eff} decreased for both complexes, due to the antiferromagnetic interactions between the two Cu ions within the dinuclear molecules. The magnetic data for **1** and [Cu₂(O₂C-*t*Bu)₄] were simulated using the Bleaney-Bowers equation:

$$\chi_M = 2[(1 - p)(Ng^2\mu_{\text{eff}}^2/kT)\{3 + \exp(-2J/kT)\}^{-1} + p(Ng^2\mu_{\text{eff}}^2/4kT) + N\alpha] \quad (1)$$

where *N* is the Avogadro's number, *g* is the spectroscopic splitting factor, β is the Bohr magneton, *k* is the Boltzmann constant, *J* is the exchange integral between the copper(II) ions, *p* is the paramagnetic mononuclear Cu(II) impurity constant, and *N* α is the temperature independent paramagnetism (TIP) [20]. The best fitting parameters, where *N* α was fixed at 60 × 10⁻⁶ cgs emu, are summarized in Table 1. The temperature-dependent profiles of magnetic susceptibilities and moments were well reproduced with the parameters for **1** and [Cu₂(O₂C-*t*Bu)₄] (Figure 3), without considering the magnetic interaction between the dicopper(II) units. This means that the interaction through the linker ligand dpybz was negligible in **1**. A negligible interaction through the axial linker ligand, pyz, was also reported for [Cu₂(O₂C-*t*Bu)₄(pyz)] and [Cu₂(O₂C-Ph)₄(pyz)], and the estimated *J* value of -175.3 cm⁻¹ for **1** was comparable to those for [Cu₂(O₂C-*t*Bu)₄(pyz)] (*J* = -183 cm⁻¹) and [Cu₂(O₂C-Ph)₄(pyz)] (*J* = -169.5 cm⁻¹) [12,13]. The *J* value of **1** (-175.3 cm⁻¹) was smaller than that of [Cu₂(O₂C-*t*Bu)₄] (*J* = -201.4 cm⁻¹), which was theoretically interpreted using DFT calculations (See Section 2.4).

Table 1. Best fitting magnetic parameters of **1** and [Cu₂(O₂C-*t*Bu)₄].

Magnetic Parameters	1	[Cu ₂ (O ₂ C- <i>t</i> Bu) ₄]
<i>J</i> (cm ⁻¹)	-175.3	-201.4
<i>g</i>	2.09	2.17
<i>N</i> α (cm ³ mol ⁻¹)	60 × 10 ⁻⁶	60 × 10 ⁻⁶
<i>p</i>	0.0039	0.00088
^a <i>R</i> /10 ⁴	4.41	3.76

$$^a R = \sum(\chi_{\text{exp}} - \chi_{\text{calcd}})^2 / \sum \chi_{\text{exp}}^2.$$

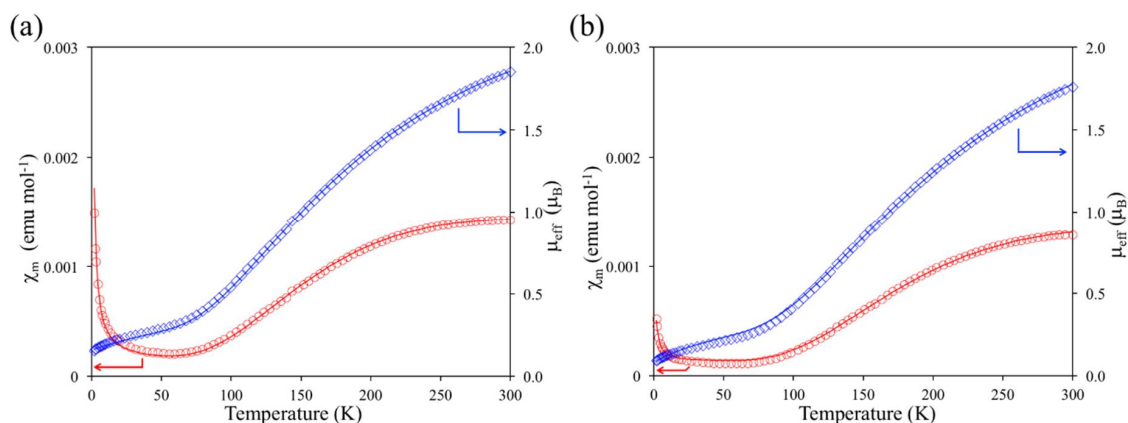


Figure 3. Magnetic susceptibilities (χ_M : \circ) and effective magnetic moments (μ_{eff} : \diamond) of (a) **1** and (b) $[\text{Cu}_2(\text{O}_2\text{C}-t\text{Bu})_4]$. Solid lines are drawn with parameter values described in the text.

2.4. Results of Theoretical Calculations

To investigate the thermodynamically favorable spin states, electronic structures, spin density distributions and magnetic properties of **1**, broken-symmetry density functional theory (BS-DFT) calculations were performed on model structures of **1**, which were obtained from crystal structures of **1**. Here, $[\text{Cu}_2(\text{O}_2\text{C}-t\text{Bu})_4]$ was also calculated for comparison. Single point energy calculations revealed that the singlet spin states of **1** and $[\text{Cu}_2(\text{O}_2\text{C}-t\text{Bu})_4]$ were 0.503 and 0.619 kcal/mol, which were more stable than their triplet spin states, indicating that **1** and $[\text{Cu}_2(\text{O}_2\text{C}-t\text{Bu})_4]$ showed antiferromagnetic coupling between the two magnetic centers in **1** and $[\text{Cu}_2(\text{O}_2\text{C}-t\text{Bu})_4]$. In fact, the calculated J values of **1** and $[\text{Cu}_2(\text{O}_2\text{C}-t\text{Bu})_4]$, which were estimated by an approximate spin-projection (AP) scheme developed by Yamaguchi's group [21], were -174.5 and -214.2 cm⁻¹, respectively. These are consistent with the experimental values for **1** and $[\text{Cu}_2(\text{O}_2\text{C}-t\text{Bu})_4]$ and are clear evidence of the antiferromagnetic interaction in **1** and $[\text{Cu}_2(\text{O}_2\text{C}-t\text{Bu})_4]$. The origin of the antiferromagnetic coupling interactions in **1** and $[\text{Cu}_2(\text{O}_2\text{C}-t\text{Bu})_4]$ were further investigated with respect to the spin density distributions. As shown in Figure 4, the spin density distributions of **1** and $[\text{Cu}_2(\text{O}_2\text{C}-t\text{Bu})_4]$ in the singlet and triplet spin states are commonly localized on the $[\text{Cu}_2(\text{O}_2\text{C}-t\text{Bu})_4]$ unit, and the singlet and triplet spin states differ only by the phases of the dx^2-y^2 orbitals of the Cu ions. Moreover, the spin densities of the dpybz moieties were negligible. The calculated results are summarized: (i) an antiferromagnetic interaction occurred in **1** between unpaired electrons residing in dx^2-y^2 orbitals of Cu ions via a super-exchange mechanism through four bridging carboxylate ligands, and (ii) the magnetic interaction between two Cu_2 units through the dpybz ligand was negligible.

Additionally, the formation of interchain CH- π interactions in the crystal structure of **1** was confirmed by long-range and dispersion corrected density functional theory (LC-DFT-D; B3LYP-D2 functional). Figure S2 shows the calculated models of two dpybz moieties, which were obtained from the crystal structure of **1**. The counterpoise method afforded an electrostatic interaction energy of -10.46 kcal/mol (-5.23 kcal/mol per CH- π interaction). This confirmed that two-fold CH- π interactions were formed between two dpybz ligands, and these were stronger than typical CH- π interactions.

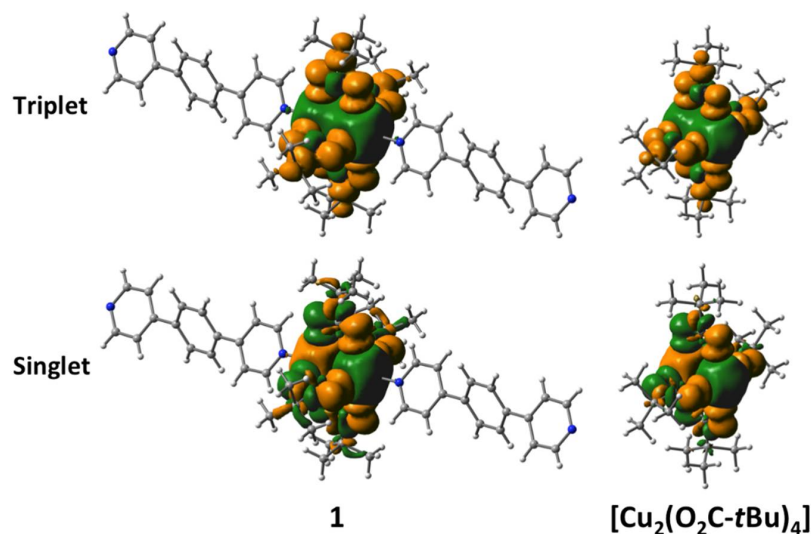


Figure 4. Spin density distributions of model structures of **1** and $[\text{Cu}_2(\text{O}_2\text{C}-t\text{Bu})_4]$ (optimized geometry at a singlet state) calculated by the uCAM-B3LYP method (basis sets: TZVP for Cu atom and 6-31+G* for other atoms).

2.5. Nitrogen Adsorption Properties

Finally, to evaluate the porosity of **1**, the nitrogen adsorption isotherm was measured at 77.4 K. As shown in Figure 5, **1** strongly adsorbed N_2 gases at a low relative pressure ($P/P_0 < 0.2$), and an arched adsorption isotherm was obtained. This type of the isotherm plot is frequently observed in physical N_2 adsorption of porous materials with micro- and subnano-pores [22] and can be classified as an IUPAC-I type isotherm. At a relative pressure of 0.3, N_2 gas was moderately adsorbed on the surface of **1**, as with typical CPs and MOFs. The Langmuir and BET surface areas of **1** were estimated as 538.0 and 400.5 m^2/g , respectively, indicating that **1** had permanent porosity even after evacuation of guest solvents from its pores. The surface area of **1** was relatively higher in one-dimensional CPs.

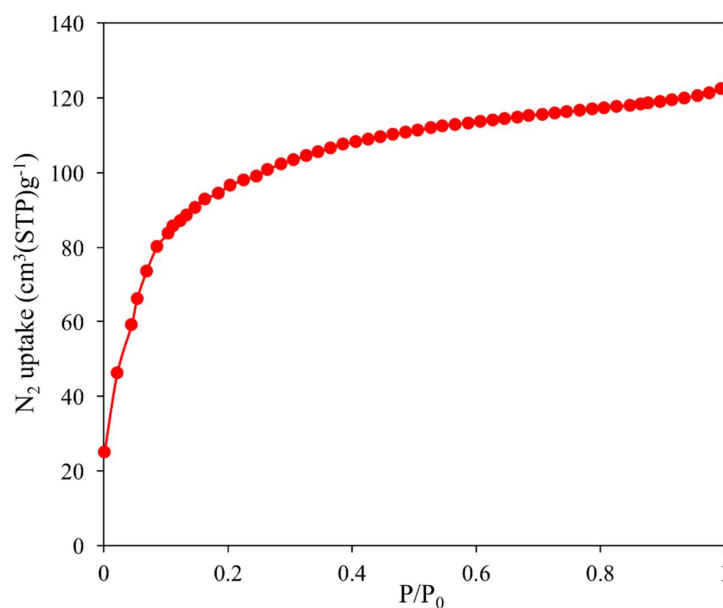


Figure 5. Nitrogen adsorption isotherm of **1** at 77.4 K.

3. Materials and Methods

3.1. General

All chemicals and solvents used in this study were purchased from commercial suppliers and were used without further purification. Fourier transform infrared (FT-IR) spectra were recorded on a JASCO FT-IR 4600 spectrophotometer using KBr pellets. Elemental analysis was conducted with a Yanaco CHN Corder MT-6 instrument. The dependence of the magnetic susceptibility on the temperature was determined using a Quantum Design MPMS magnetometer at 5000 Oe from 2 to 300 K. The nitrogen adsorption isotherm of **1** was measured at 77.4 K with a MicrotracBEL BELSORP-mini II analyzer.

3.2. Single Crystal X-ray Diffraction

Single crystals suitable for single crystal X-ray diffraction were obtained by using the method described in Section 3.5. A crystal of **1** was coated in Parabar oil to protect it from moisture, mounted on a CryoLoop and placed on a goniometer head. X-ray diffraction data for **1** were collected at 150 K on a RIGAKU Mercury 70 CCD system equipped with a rotating anode X-ray generator with monochromated Mo- $K\alpha$ radiation ($\lambda = 0.71075 \text{ \AA}$). Diffraction data for **1** were processed using the CrystalClear-SM program (RIGAKU). The structure of **1** was initially solved with a direct method (SIR-2011) [23] and refined using the full-matrix least-squares technique F^2 with SHELXL-2014 [24] in the CrystalStructure 4.2.5 software (RIGAKU). Non-hydrogen atoms were refined with anisotropic displacement parameters, and hydrogen atoms were located in the calculated positions and refined using riding models. The residual electron densities in the void space of the final refined structure of **1** were evaluated using the PLATON SQUEEZE program [18]. The crystal data can be obtained as Crystallographic information file (CIF) from the Cambridge Crystallographic Data Center (CCDC). The deposition number of **1** was 1841609.

3.3. Theoretical Calculation

The BS-DFT calculations performed in this study were carried out with a long-range corrected uCAM-B3LYP functional [25] combined with the TZVP basis set for Cu and 6-31+G* for other atoms in the Gaussian 09 program [26]. The geometry of the calculated model of **1** was obtained from its crystal structure, while that of $[\text{Cu}_2(\text{O}_2\text{C}-t\text{Bu})_4]$ was obtained by full geometry optimization in the singlet state. The exchange integral (J) was estimated by the AP scheme (known as the Yamaguchi equation; see Scheme 2) developed by Yamaguchi's group [21]:

$$J = \frac{E_{\text{singlet}} - E_{\text{triplet}}}{\langle S^2 \rangle_{\text{singlet}} - \langle S^2 \rangle_{\text{triplet}}} \quad (2)$$

where E and $\langle S^2 \rangle$ are the total energy and total angular momentum, respectively. The interchain CH- π interaction in the crystal structure of **1** was evaluated with the long-range and dispersion corrected CAM-B3LYP-D2 functional combined with the 6-31+G* basis set. Here, the counterpoise method was applied to estimate the energies of the CH- π interaction. Spin density distributions were drawn using the GaussView program.

3.4. Synthesis of $[\text{Cu}_2(\text{O}_2\text{C}-t\text{Bu})_4]$

$[\text{Cu}_2(\text{O}_2\text{C}-t\text{Bu})_4]$ was prepared by a literature method with slight modifications [27]. A mixture of $[\text{Cu}_2(\text{O}_2\text{CCH}_3)_4(\text{H}_2\text{O})_2]$ (159.8 mg, 0.400 mmol) and pivalic acid (5.0 mL, 0.044 mol) in EtOH (30.0 mL) was heated at 323 K for 2 h. The resulting solution was evaporated to dryness, and its residue was collected on a membrane filter and washed with hexane. The obtained blue powder was dried under vacuum at 353 K for 3 h. $[\text{Cu}_2(\text{O}_2\text{C}-t\text{Bu})_4]$ was obtained as a crystalline blue powder in 79.9% (170.0 mg)

yield. Anal. Calcd for $C_{20}H_{36}Cu_2O_8$: C, 45.19; H, 6.83%. Found: C, 45.19; H, 6.67%. IR data (KBr disk, cm^{-1}): 1578 (s), 1529 (w), 1484 (w), 1418 (m), 1377 (w), 1362 (w), 1226 (m), 897 (w), 786 (w) and 624 (vw).

3.5. Synthesis of $[Cu_2(O_2C-tBu)_4(dpybz)]$ (**1**)

A THF solution (7.0 mL) of $[Cu_2(O_2C-tBu)_4]$ (79.7 mg, 0.15 mmol) and a DMF solution (10.0 mL) of dpybz (34.8 mg, 0.15 mmol) were mixed and left for 10 days at room temperature. The single crystals deposited at the bottom of the flask were collected on a membrane filter, washed with DMF and diethylether, and finally dried at 353 K under vacuum for 3 h. **1** was obtained as a crystalline green powder in 80.0% (89.8 mg) yield. Anal. Calcd for $C_{36}H_{48}Cu_2N_2O_8$: C, 56.61; H, 6.33; N, 3.67%. Found: C, 56.86; H, 6.09; N, 3.88%. IR data (KBr disk, cm^{-1}): 2958 (m), 2926 (w), 2871 (w), 1617 (s), 1607 (s), 1483 (m), 1418 (m), 1376 (w), 1361 (w), 1226 (m), 810 (w), 789 (w), 717 (w) and 619 (w).

4. Conclusions

In conclusion, we investigated the synthesis, crystal structure, and magnetic and gas-adsorption properties of a one-dimensional chain-type Cu_2 coordination polymer, **1**, by means of experimental and theoretical techniques. Single crystal X-ray diffraction revealed that (i) the $[Cu_2(O_2C-tBu)_4]$ SBU and dpybz ligand were alternately arranged to create the one-dimensional chain-type structure of **1**, and (ii) interchain CH- π interactions of the dpybz moieties of **1** played an important role in forming the self-assembled brick-like porous network structures of **1**. From these results, enlarging the planarity of dpybz was considered to stabilize the self-assembled structures of CPs and MOFs via electrostatic interactions. Magnetic analyses and DFT calculations confirmed that antiferromagnetic interactions were present between the two Cu ions through bridging carboxylate ligands, and that the magnetic interaction between two Cu_2 units through the dpybz ligand was negligible. The N_2 adsorption measurements confirmed that the porous network structure of **1** was maintained even after evacuation of guest solvent molecules from its pores, and **1** adsorbed a suitable amount of N_2 gas into its pores. Thus, **1** is an exceptional example of a robust porous network CP, which is maintained by electrostatic CH- π interactions.

Supplementary Materials: The following are available online at <http://www.mdpi.com/2312-7481/4/2/26/s1>. Figure S1: IR spectrum of **1** (in KBr) at 300 K. Figure S2: Calculated model structures of two dpybz ligands. Table S1: Crystallographic data of **1**. Table S2: Selected bond lengths (\AA) and angles ($^\circ$) of the crystal structure of **1**.

Author Contributions: N.Y. performed the experiments and wrote the paper; M.H. analyzed the data; M.M. contributed analysis tools and performed the gas-adsorption experiments; Y.K. conceived and designed the experiments, analyzed the data and wrote the paper.

Funding: This work was partially supported by Grant-in-Aid for Scientific Research Nos. 15K17897, 16K05722, and 17J11019 from the Ministry of Education, Culture, Sports, Science and Technology (MEXT), Japan.

Acknowledgments: N.Y. acknowledges Research Fellowships of Japan Society for the Promotion of Science for Young Scientists.

Conflicts of Interest: The authors declare no conflicts of interest.

References

1. Van Nierkert, J.N.; Schoening, F.R.L. X-ray Evidence for Metal-to-Metal Bonds in Cupric and Chromous Acetate. *Nature* **1953**, *171*, 6834–6859. [[CrossRef](#)]
2. Melnik, M. Study of the relation between the structural data and magnetic interaction in oxo-bridged binuclear copper(II) compounds. *Coord. Chem. Rev.* **1982**, *42*, 259–293. [[CrossRef](#)]
3. Kato, M.; Muto, Y. Factors affecting the magnetic properties of dimeric copper(II) complexes. *Coord. Chem. Rev.* **1988**, *92*, 45–83. [[CrossRef](#)]

4. Köberl, M.; Cokoja, M.; Herrmann, W.A.; Kühn, F.E. From molecules to materials: Molecular paddle-wheel synthons of macromolecules, cage compounds and metal-organic frameworks. *Dalton Trans.* **2011**, *40*, 6834–6859. [[CrossRef](#)] [[PubMed](#)]
5. Eddaoudi, M.; Kim, J.; Wachter, J.B.; Chae, H.K.; O'Keeffe, M.; Yaghi, O.M. Porous Metal-Organic Polyhedra: 25 Å Cuboctahedron Constructed from 12 Cu₂(CO₂)₄ Paddle-Wheel Building Blocks. *J. Am. Chem. Soc.* **2001**, *123*, 4368–4369. [[CrossRef](#)] [[PubMed](#)]
6. Rao, V.M.; Sathyanarayana, D.N.; Manohar, H. X-ray crystal structures of some adducts of dimeric copper(II) acetate. Nature of the copper-copper interaction. *J. Chem. Soc. Dalton Trans.* **1983**, *0*, 2167–2173. [[CrossRef](#)]
7. Horikoshi, R.; Mikuriya, M. One-Dimensional Coordination Polymers from the Self-Assembly of Copper(II) Carboxylates and 4,4'-Dithiobis(pyridine). *Bull. Chem. Soc. Jpn.* **2005**, *78*, 827–834. [[CrossRef](#)]
8. Mori, W.; Inoue, F.; Yoshida, K.; Nakayama, H.; Takamizawa, S.; Kishita, M. Synthesis of New Adsorbent Copper(II) Terephthalate. *Chem. Lett.* **1997**, *26*, 1219–1220. [[CrossRef](#)]
9. Chui, S.S.-Y.; Lo, S.M.-F.; Charmant, J.P.H.; Orpen, A.G.; Williams, I.D. A Chemically Functionalizable Nanoporous Material [Cu₃(TMA)₂(H₂O)₃]_n. *Science* **1999**, *283*, 1148–1150. [[CrossRef](#)] [[PubMed](#)]
10. Seki, K.; Takamizawa, S.; Mori, W. Design and Gas Adsorption Property of a Three-Dimensional Coordination Polymer with a Stable and Highly Porous Framework. *Chem. Lett.* **2001**, *30*, 332–333. [[CrossRef](#)]
11. Ohmura, T.; Usuki, A.; Fukumori, K.; Ohta, T.; Ito, M.; Tatsumi, K. New-Porphyrin-Based Metal-Organic Framework with High Porosity: 2-D Infinite 22.2 Å Square-Grid Coordination Network. *Inorg. Chem.* **2006**, *45*, 7988–7990. [[CrossRef](#)] [[PubMed](#)]
12. Mikuriya, M.; Nukada, R.; Morishita, H.; Handa, M. Chain Compounds Formed by the Reaction of Copper(II) Carboxylate [Cu₂(O₂CR)₄] (R = C(CH₃)₃, CCl₃) and Bridging Ligand L (L = Pyrazine, 4,4'-Bipyridine, and 1,4-Diazabicyclo[2,2,2]octane). *Chem. Lett.* **1995**, *24*, 617–618. [[CrossRef](#)]
13. Nukada, R.; Mori, W.; Takamizawa, S.; Mikuriya, M.; Handa, M.; Naono, H. Microporous Structure of a Chain Compound of Copper(II) Benzoate Bridged by Pyrazine. *Chem. Lett.* **1999**, *28*, 367–368. [[CrossRef](#)]
14. Takahashi, K.; Hishino, N.; Takeda, T.; Noro, S.; Nakamura, T.; Takeda, S.; Akutagawa, T. Structural Flexibilities and Gas Adsorption Properties of One-Dimensional Copper(II) Polymers with Paddle-Wheel Units by Modification of Benzoate Ligands. *Inorg. Chem.* **2015**, *54*, 9423–9431. [[CrossRef](#)] [[PubMed](#)]
15. Hwang, I.J.; Jo, Y.D.; Kim, H.; Kim, K.B.; Jung, K.-D.; Kim, C.; Kim, Y.; Kim, S.-J. Catalytic transesterification reactions of one-dimensional coordination polymers containing paddle-wheel-type units connected by various bridging ligands. *Inorg. Chim. Acta* **2013**, *402*, 39–45. [[CrossRef](#)]
16. Liu, C.-S.; Wang, J.-J.; Yan, L.-F.; Chang, Z.; Bu, X.-H.; Sañudo, E.C.; Ribas, J. Copper(II), Cobalt(II), and Nickel(II) Complexes with a Bulky Anthracene-Based Carboxylate Ligand: Synthesis, Crystal Structures, and Magnetic Properties. *Inorg. Chem.* **2007**, *46*, 6299–6310. [[CrossRef](#)] [[PubMed](#)]
17. Kataoka, Y.; Yano, N.; Shimodaira, T.; Yan, Y.-N.; Yamasaki, M.; Tanaka, H.; Omata, K.; Kawamoto, T.; Handa, M. Paddlewheel-Type Dirhodium Tetrapivalate Based Coordination Polymer: Synthesis, Characterization, and Self-Assembly and Disassembly Transformation Properties. *Eur. J. Inorg. Chem.* **2016**, *17*, 2810–2815. [[CrossRef](#)]
18. Tsuzuki, S.; Fujii, A. Nature and physical origin of CH/π interaction: Significant difference from conventional hydrogen bonds. *Phys. Chem. Chem. Phys.* **2008**, *19*, 2584–2594. [[CrossRef](#)] [[PubMed](#)]
19. Spek, A.L. Structure validation in chemical crystallography. *Acta Crystallogr.* **2009**, *D65*, 148–155. [[CrossRef](#)] [[PubMed](#)]
20. Bleaney, B.; Bowers, K.D. Anomalous paramagnetism of copper acetate. *Proc. R. Soc. A* **1952**, *214*, 451–465. [[CrossRef](#)]
21. Yamaguchi, K.; Tsunekawa, T.; Yoyoda, Y.; Fueno, T. Ab initio molecular orbital calculations of effective exchange integrals between transition metal ions. *Chem. Phys. Lett.* **1988**, *143*, 371–376. [[CrossRef](#)]
22. An, J.; Fiorella, R.P.; Geib, S.J.; Rosi, N.L. Synthesis, Structure, Assembly, and Modulation of the CO₂ Adsorption Properties of a Zinc-Adeninate Macrocycle. *J. Am. Chem. Soc.* **2009**, *131*, 8401–8403. [[CrossRef](#)] [[PubMed](#)]
23. Buria, M.C.; Caliendo, R.; Camalli, M.; Carrozzini, B.; Cascarano, G.L.; Giacobozzo, C.; Mallamo, M.; Mazzone, A.; Polodori, G.; Spagna, R. SIR2011: A new package for crystal structure determination and refinement. *J. Appl. Cryst.* **2012**, *45*, 357–361.

24. Sheldrick, G.M. Crystal structure refinement with SHELXL. *Acta Crystallogr.* **2015**, *C71*, 3–8. [[CrossRef](#)]
25. Yanai, T.; Tew, D.P.; Handy, N.C. A new hybrid exchange-correlation functional using the Coulomb-attenuating method (CAM-B3LYP). *Chem. Phys. Lett.* **2004**, *393*, 51–57. [[CrossRef](#)]
26. Frisch, M.J.; Trucks, G.W.; Schlegel, H.B.; Scuseria, G.E.; Robb, M.A.; Cheeseman, J.R.; Scalmani, G.; Barone, V.; Mennucci, B.; Petersson, G.A.; et al. *Gaussian 09, Revision C.01*; Gaussian, Inc.: Wallingford, CT, USA, 2009.
27. Muto, Y.; Hirashima, N.; Tokii, T.; Kato, M.; Suzuki, I. Magnetic Properties of Dimeric Copper(II) 2,2-Dimethylpropanoate. *Bull. Chem. Soc. Jpn.* **1986**, *589*, 3672–3674. [[CrossRef](#)]



© 2018 by the authors. Licensee MDPI, Basel, Switzerland. This article is an open access article distributed under the terms and conditions of the Creative Commons Attribution (CC BY) license (<http://creativecommons.org/licenses/by/4.0/>).